

An Electrochemical Sensor for Determination of Ceftazidime Based on Poly (crystal violet) Doped Platinum Nanoparticles Modified Electrode

Yanli Sun, Xin Li, Xueliang Wang^{*}, Zhangyu Yu, Tao Wang^{*}

Department of Chemistry and Chemical Engineering, Heze University, Heze 274015, People's Republic of China

^{*}E-mail: yuzywxl@163.com

Received: 2 October 2017 / *Accepted:* 1 December 2017 / *Published:* 28 December 2017

An electrochemical sensor for determination of ceftazidime (CFD) was fabricated by polymerizing crystal violet (PCV) and platinum nanoparticles (nanoPt) on a glassy carbon electrode (GCE). The nanoPt/PCV composite film exhibited excellent catalytic performance toward CFD. On this modified electrode, the CFD had an irreversible oxidation peak at 0.8 V with a dramatically amplified current value. The electrochemical behaviors of CFD and the conditions that may affect these behaviors were investigated detailedly on the nanoPt/PCV/GCE. Under the optimized conditions, the sensor showed a wide linear range over the concentration of CFD from 0.25 to 10 μM . The detection limit was 0.01 μM . The sensor can be applied for detecting the content of CFD in meat samples with good selectivity and stability. The recovery was between 97.8% and 103%.

Keywords: Electrochemical sensor; Ceftazidime; Crystal violet; Pt nanoparticle; Application

1. INTRODUCTION

Ceftazidime (CFD, Fig. 1) is a kind of cephalosporin antibiotic. It is highly stable to most of β -lactamases produced by gram-negative and gram-positive bacteria [1]. CFD has been widely used in the treatment of susceptible infections including respiratory-tract infections, such as pneumonia and lung infections, skin and soft tissue infections, and other many abdominal infections [2]. Due to its excellent control effect, CFD is also applied to poultry breeding to prevent and cure animal's disease. In the past years, this application has made a great contribution to the development of poultry husbandry industry [3, 4]. However, its use inevitably leads to antibiotics residue in meat food, and these antibiotics residue can be accumulated in body after long-term consumption and threaten to

human's health [5, 6]. So the detection of CFD residues in meat food has attracted more and more attentions from society and researchers.

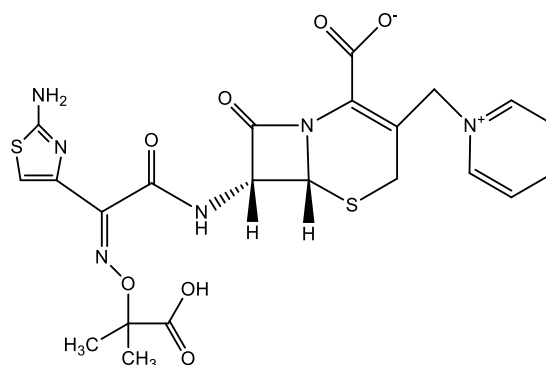


Figure 1. The structure of Ceftazidime (CFD)

Several analytical methods, including high performance liquid chromatography [7, 8], electrophoretic [9-11], fluorescent method [12-14] and electrochemical methods [15, 16] have been used for the detection of CFD. Among of these analytical methods, electrochemical methods, especially the electrochemical biosensors, have been regarded as effective tools for determination of antibiotics with easy, fast, simple operation, low cost advantages [17, 18]. To the best of our knowledge, the electrochemical sensors that have been reported are mainly focusing on determination of CFD in pharmaceutical and clinical preparations [15, 16]. The determination of CFD residue in meat food has rarely been reported.

In order to fabricate a modified electrode with unique superiority in high sensitivity, selectivity, reproducibility and stability, the electrochemical polymerization have been extensively used in preparing modified electrode [19, 20]. Metal nanomaterials, such as platinum and gold, have also been widely used in electrochemical field on account of their good electronic conductivity, catalytic activity, good chemical stability and chemical inertness [21-24].

Here, crystal violet and platinum nanoparticles were successively electro-polymerized on a glassy carbon electrode surface with a cyclic voltammetry. The modified electrode was applied to investigate the electrochemical behaviors of CFD and to detect the residue of CFD in meat food.

2. EXPERIMENT

2.1 Reagents and Apparatus

The concentration of 1.0×10^{-3} M CFD (Dalian Mellon biological technology co., LTD, China), 1.0×10^{-4} M crystal violet (Guangzhou Chemical Reagent Factory, China) and 2.0 mM H₂PtCl₆ (Shanghai FanKe biological technology co., LTD, China) standard solutions were respectively prepared in purified water. All other reagents of analytical grade were purchased from civil chemical

reagent corporation. Ultrapure water from a KJY1002-UVF water prepared system was used throughout the experiments. All experiments were performed at room temperature.

All electrochemical measurements were conducted on a CHI660D electrochemical workstation (Shanghai Chenhua Co., China). A traditional three-electrode system was employed, with a modified electrode as working electrode, a saturated calomel electrode as a reference electrode and platinum wires as an auxiliary electrode. Scanning electron microscope (SEM) image was from a field emission SEM Sirion 200 (FEI, America). Sonication was conducted using a KQ-600 ultrasonic cleaner (Kunshan, China), and acidity was measured by a PHS-3G Precision pH meter (Shanghai, China).

2.2 Preparation of modified electrode

A bare glassy carbon electrode (3 mm in diameter) was polished with abrasive paper and alumina power plasma in sequence, and then was sonicated in $\text{HNO}_3(1:1, \text{V/V})$, ethanol, distilled water respectively. After washing with water, the electrode was put into a beaker containing 12.0 mL $\text{pH} = 4.0$ of phosphate buffer solution (PBS), 2.0 mL 1.0×10^{-4} M crystal violet solution and 6.0 mL 1.0 M KNO_3 solution. The PCV/GCE electrode was obtained by a cyclic voltammetry at a scanning rate of $100 \text{ mV} \cdot \text{s}^{-1}$ in a potential range from 0 to 1.2 V for 10 cycles. Then, the nanoparticle platinum was modified on the electrode in 2.0 mM H_2PtCl_6 solution with same cyclic voltammetry method to get a nanoPt/PCV/GCE modified electrode.

2.3 Electrochemical measurement

A certain amount of 1.0×10^{-3} M CFD standard solution was mixed with PBS of $\text{pH} 4.0$ in a 20.0 mL electrolytic cell. The cyclic scans were conducted at a scan rate of $100 \text{ mV} \cdot \text{s}^{-1}$ in the potential range between 0.5 and 1.1 V with three-electrode system.

3. RESULTS AND DISCUSSION

3.1 The morphology of the modified electrode

In order to verify the electrode has been modified successively, the morphology of the modified electrode surface was investigated by scanning electron microscopy (SEM) (Fig. 2). Fig. 2 A and Fig. 2 B are the SEM images of bare GCE and nanoPt/PCV/GCE, respectively. After the crystal violet and platinum nanoparticles were electropolymerized on the glassy carbon electrode surface, a layer of membrane with many bright spots (the red circle marked) were observed, revealing that poly crystal violet and platinum nanoparticles were successfully modified on the surface.

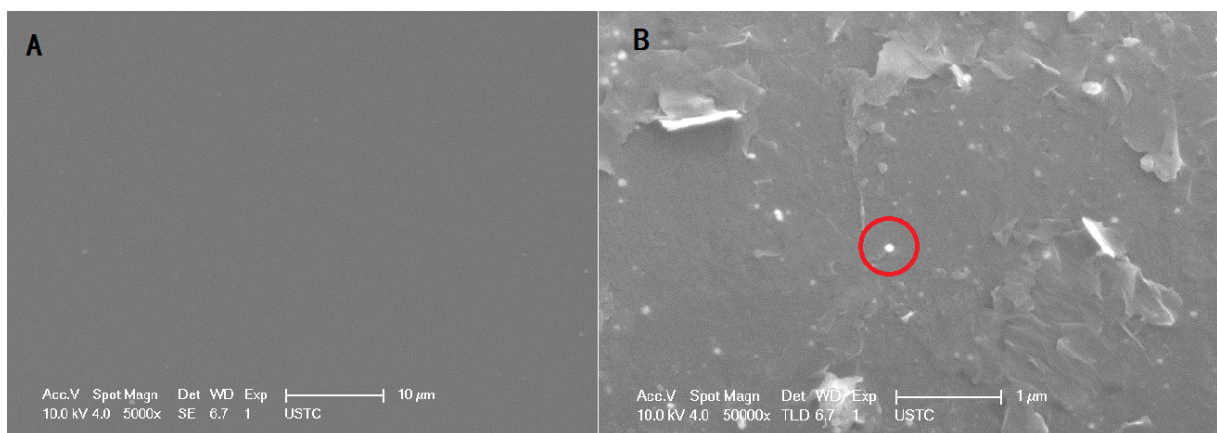


Figure 2. SEM images of the bare GCE (A) and nanoPt/PCV/GCE (B)

3.2 Electrochemical behaviors of CFD

The electrochemical behaviors of CFD were respectively investigated by cyclic voltammetry (CV) at a bare GCE, PCV/GCE and nanoPt/PCV/GCE (Fig. 3). As can be seen from the curve a, CFD had almost no electrochemical response on a bare GCE. When the PCV was modified on the GCE surface, CFD had an oxidation peak current at about 0.82 V and no reduction peak current appeared (curve b), the results are consistent with the reference of [25]. The electrochemical reaction of CFD on the PCV/GCE was an irreversible process. On the nanoPt/PCV/GCE, the oxidation current value of CFD was significantly improved compared with that at the other two electrodes, and the peak potential shifted to 0.8 V simultaneously, which revealed that the nanoPt/PCV film has catalytic activity toward the electrochemical reaction of the CFD.

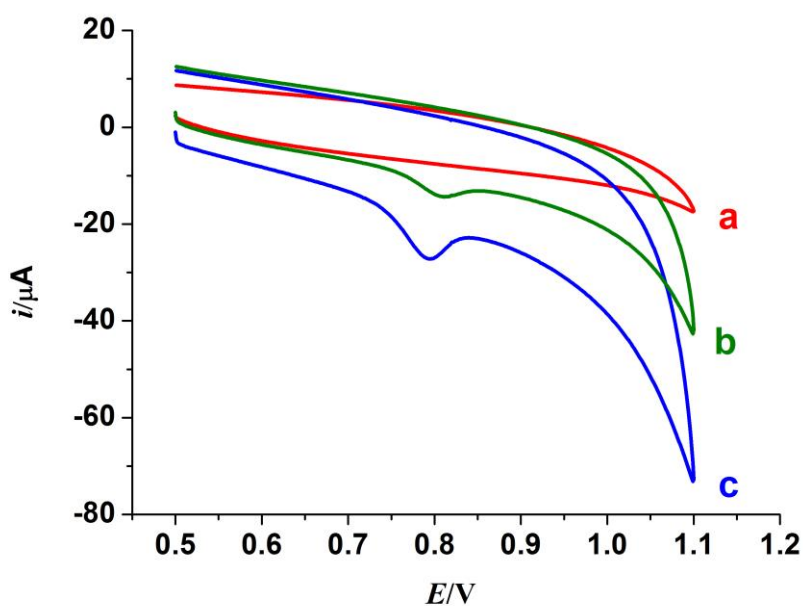


Figure 3. Cyclic voltammograms of 5.0×10^{-6} M CFD on a bare GCE(a), PCV/GCE(b) and NanoPt/PCV/GCE(c) in pH 4.0 PBS with a scan rate of $100.0 \text{ mV} \cdot \text{s}^{-1}$

3.3 Optimizing the conditions for determination of CFD

3.3.1 The optimal pH of PBS

To investigate the pH effect of PBS on the electrochemical signals of CFD, the PBS in a variety of pH was prepared. The pH of PBS had obviously influence on the redox reaction of CFD at the nanoPt/PCV/GCE modified electrode in pH range from 2.2 to 7.0 (Fig. 4). The peak current reached its maximum value when the pH of PBS was 4.0, therefore, the PBS of pH 4.0 was chosen as the supporting electrolyte. In the reference of [25], the optimal pH value is 5.0.

Meanwhile, the oxidation peaks shifted negatively with the increase of the pH values, and a linear relationship was obtained between the oxidation peak potentials (E) and pH values $E(V) = 1.06 - 0.060 \text{ pH}$, $R = 0.9986$ (the inset of Fig. 4). According to the Nernst Equation, we can deduce that the equal sum of electrons and protons were involved in the reactions from the slope value of 0.060.

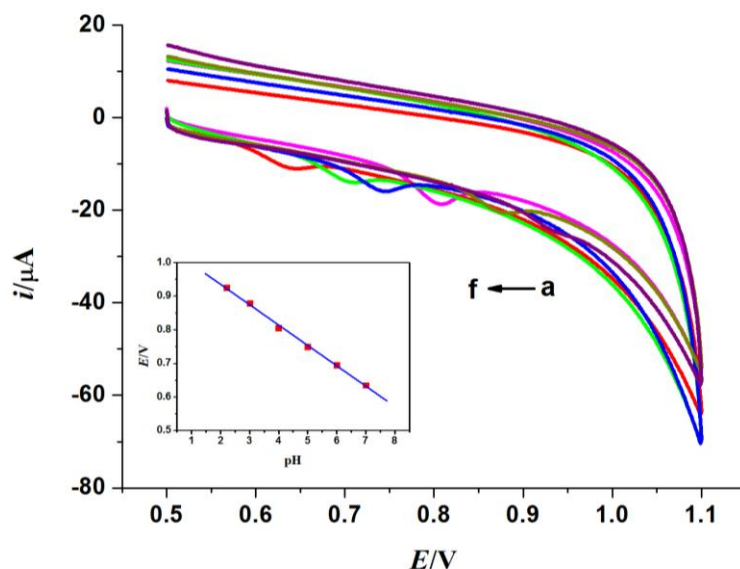


Figure 4. Cyclic voltammograms of 5.0×10^{-6} M CFD on nanoPt/PCV/GCE in different pHs (a→f: 2.2, 3.0, 4.0, 5.0, 6.0, 7.0) with a $100 \text{ mV} \cdot \text{s}^{-1}$ scan rate. The inset: the plot of peak potentials versus pHs

3.3.2 The optimal scan rates

Fig. 5 showed the influence of the scan rates on the electrochemical behaviors of CFD in the scan rate range of $20\text{--}220 \text{ mV} \cdot \text{s}^{-1}$. We can see that the oxidation potential (E) shifted positively and the peak currents linearly increased with the increase of the scan rates. That is because the quantity of hydroxyl radical generated on the surface of the anode increased with the increase of the scan rates, whereas the oxidation of ceftazidime on the anode was affected by hydroxyl radicals [26]. The linear regression equation can be expressed as $I (\text{mA}) = -0.216 + 0.089v (\text{mV} \cdot \text{s}^{-1})$, $R = 0.9985$, which showed that the oxidation processes of CFD at the modified electrode is adsorption controlled processes. However, on the Pd–Au nanoparticle decorated carbon nanotube modified electrode, the peak current

is linearly with the square root of the sweep rate, showing the oxidation processes of CFD is the diffusion-controlled process[25].

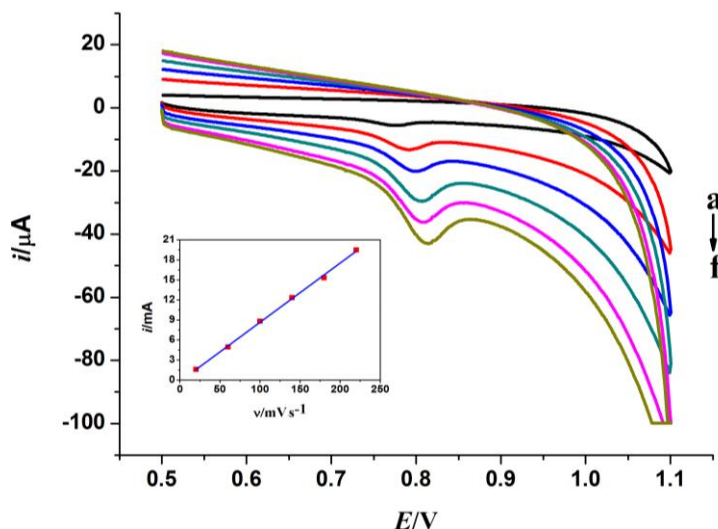


Figure 5. Cyclic voltammograms of 5.0×10^{-6} M CFD on the nanoPt/PCV/GCE in pH 4.0 PBS with scan rates of 20.0, 60.0, 100.0, 140.0, 180.0 and 220.0 $\text{mV} \cdot \text{s}^{-1}$ respectively (from curve a to f). Inset: the plot of the peak currents versus the scan rates

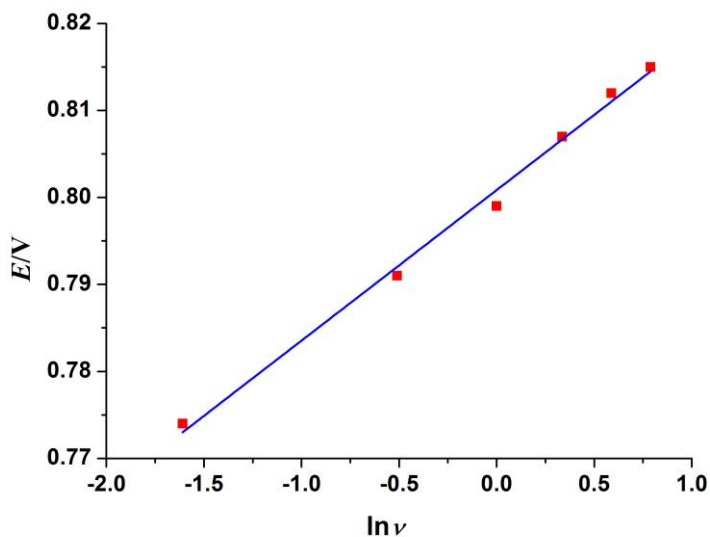


Figure 6. The linear relationship of *E* and $\ln v$

The relationship of the oxidation potential (*E*) with the $\ln v$ was also investigated and the results were showed in Fig. 6. The plot of *E* vs. $\ln v$ can be expressed with the equation of E (V) = 0.0173 $\ln v$ ($\text{mV} \cdot \text{s}^{-1}$) + 0.801, $R = 0.9921$. According to equation of Laviron [27]:

$$E = E_0 + \frac{RT}{anF} \ln \frac{RTk_s}{anF} - \frac{RT}{anF} \ln v \quad (1)$$

Where n is the number of electron transferred and α is the electron transfer coefficient, k_s is the apparent heterogeneous electron transfer rate constant. In most systems, α turns out to be between 0.3 and 0.7, and can be regarded as 0.5 in ideal condition, so the $n = 5.8 \approx 6.0$ was calculated.

3.3.3 Effect of the accumulation time

Because electrochemical reaction process of CFD at the modified electrode was an adsorption-controlled process, the accumulation time may influence the electrochemical behaviors of CFD, so different accumulation time was studied. The results showed that the peak current increased as the accumulation time increased from 0 to 60 s and kept nearly unchanged when the accumulation time was further increased. Therefore, the accumulation time of 60 s was chosen in all experiments.

3.4 The analytical performances of the sensor

3.4.1 Linear range and the detection limit

The determination of CFD was carried out by a CV method. The relationship of the oxidation peak current and the concentration of CFD were shown in Fig. 7. As can be seen, the oxidation peak current increased linearly with concentration of CFD from 0.25 μM to 10.0 μM . The linear regression equation was $I (\mu\text{A}) = 1.23 + 2.17c (\mu\text{M})$, $R = 0.9956$. The detection limit was evaluated to be 0.01 μM .

Compared with other reports about CFD detection, this method has high accuracy and sensitivity with a simple and easy preparation (Table 1).

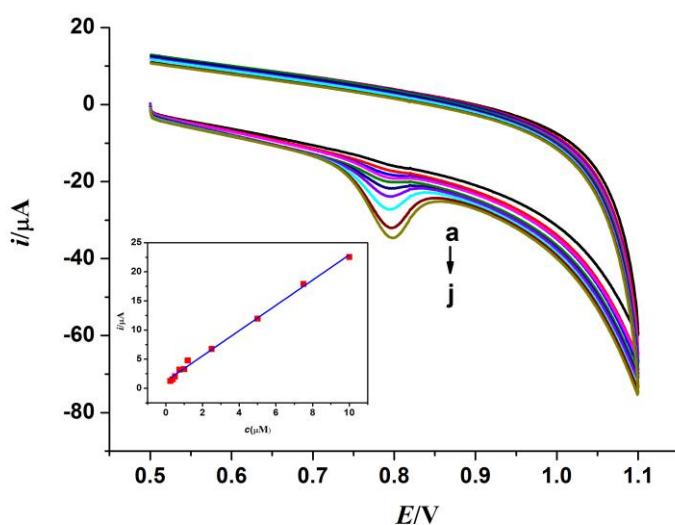


Figure 7. Cyclic voltammograms of different concentration of CFD (a→j: 0.25, 0.37, 0.50, 0.75, 1.00, 1.20, 2.50, 5.00, 7.50, 10.0 μM) on the nanoPt/PCV/GCE in pH 4.0 PBS at the scan rate of 100 $\text{mV}\cdot\text{s}^{-1}$. Inset: the plot of the peak currents versus the concentrations of CFD

Table 1. The comparison between this method and other reports

	Method	Detection limit	Linear range	sample	Recovery (%)
This article [28]	Electrochemical	0.01 μM	0.25-10 μM	chicken	97.8 -103
	HPLC-electrochemical	0.75 $\mu\text{g}\cdot\text{ml}$	5-200 $\mu\text{g}\cdot\text{ml}$	plasma	96-105.8
[16]	Electrochemical	1 nM	0.05-50 μM	blood	99.1-104.4
[9]	Electrophoretic Stacking	0.8 μM	\	blood	\

3.4.2 Reproducibility and interference test

The reproducibility was investigated by calculating the RSD of peak currents of 5.0×10^{-6} M CFD on five different modified electrodes that were fabricated independently with same procedures. The RSD of the peak currents for the five electrodes was 3.2%.

The potential interferences for determination of CFD were investigated. The results showed that there were no obviously influence on the oxidation peak of CFD in presence of 50-fold of K^+ , Na^+ , Mg^{2+} , Ca^{2+} , NO_3^- , glucose, folic acid, and 10-fold dopamine, ascorbic acid. These results indicated a good selectivity of the sensor for determination of CFD.

3.4.3 Analytical application

The electrochemical sensor based on nanoPt/PCV/GCE was used for detection of the CFD in meat food. Firstly, some chicken and duck purchased from local market was prepared and grinded with a meat grinder. Then, five grams of meat was translated to a sample tube and ultrasonication extracted for 1.0 h with 5.0 mL of methanol and acetone (4:1, V/V). After centrifuged, the supernatants were taken out and filtered through 0.45 μm membrane filter twice. The solution was then diluted with 5.0 mL pH 4.0 PBS. After that, the present method was used for the detection of CFD in the pretreated samples and no peak current was observed in the samples. Finally, all these pretreated samples were spiked with standard CFD solutions and the recovery was calculated (Tab. 1).

Table 2. Recovery measurements of the CFD in meat samples

Samples	Added (M)	Found (M)	Recovery (%)	RSD (%)
Chicken1	0.00	ND	ND	ND
	5.00×10^{-7}	4.96×10^{-7}	99.2	3.32
	1.00×10^{-6}	9.78×10^{-7}	97.8	2.97
	5.00×10^{-6}	4.99×10^{-6}	99.8	3.53
Chicken2	0.00	ND	ND	ND
	5.00×10^{-7}	5.05×10^{-7}	101	2.84
	1.00×10^{-6}	1.03×10^{-6}	103	3.02
	5.00×10^{-6}	4.98×10^{-6}	99.6	3.17
Duck	0.00	ND	ND	ND
	5.00×10^{-7}	5.02×10^{-7}	100.4	3.22
	1.00×10^{-6}	9.97×10^{-7}	99.7	3.56
	5.00×10^{-6}	4.97×10^{-6}	99.4	3.09

4. CONCLUSIONS

The modified electrode (nanoPt/PCV/GCE) was fabricated by electro-polymerizing crystal violet and platinum on a glassy carbon electrode with cyclic voltammetry, and the electrochemical behaviors of CFD at the modified electrode were investigated detailedly. CFD had an irreversible oxidation peak at 0.8V with a dramatically amplified current value on the nanoPt/PCV/GCE, which showed that the nanoPt/PCV composite film had excellent catalytic performance toward the oxidation of CFD. Meanwhile, various factors that may affect the electrochemical behaviors of nanoPt/PCV/GCE were optimized. Under the optimal conditions, the sensor showed a wide linear range over the concentration of CFD from 0.25 to 10 μM with the detection limit of 0.01 μM . Furthermore, the sensor was successfully applied to detect CFD in meat samples with good selectivity and stability, and the recovery was between 97.8% and 103%.

ACKNOWLEDGEMENTS

The work was supported by the Natural Science Foundation Committee of Shandong Province, China (No. ZR2015BL014, ZR2017MB062, BS2013HZ027), and China Postdoctoral Science Foundation Funded Project (No. 2015M572040).

References

1. J.W. Peterson, L.J. Petrasky, M.D. Seymour, R.S. Burkhart and A.B. Schuiling, *Chemosphere*, 87 (2012) 911.
2. K. Florey, *Academic Press*, San Diego, California, (1990) 95.
3. K. Kümmerer, *J. Antimicrob. Chemoth.*, 52 (2003) 5.
4. S.L. Gorbach, *New Engl. J. Med.*, 345 (2001) 1202.
5. P.É. Kjeld, *Clin. Infect. Dis.*, 41 (2011) 287.
6. O.A. Oliver, J.N. Lester, N. Voulvoulis, *Trends Biotechnol.*, 23 (2005) 163.
7. J.O. Boison, C.D. Salisbury, W. Chan, J.D. Macneil, *Associa. Officia. Analy. Chem.*, 74 (1991) 497.
8. K.L. Tyczkowska, S.S. Seay, M.K. Stoskopt, D.P. Aucoin, *J. Chromatogr. B*, 576 (1992) 305.
9. P. Tůma, M. Jaček, V. Fejfarová, J. Polák, *Anal. Chim. Acta*, 942 (2016) 139.
10. C.L. Flurer, *Electrophoresis*, 18 (1997) 2427.
11. C. García-Ruiz, M.L. Marina, *Electrophoresis*, 27 (2006) 266.
12. J. Yang, Q. Ma, X. Wu, L. Sun, X. Cao, *Anal. Lett.*, 32 (1999) 471.
13. N.P. Gutiérrez, B.A. El, R.E. Rodríguez, *Analyst*, 123 (1998) 2263.
14. P.G. Navarro, A.E. Bekkouri, E.R. Reinoso, *Biomed. Chromatogr.*, 13 (2015) 105.
15. X. Hu, Y. Yu, Z. Sun, *Electrochim. Acta*, 199 (2016) 80.
16. S. Shahrokhian, R. Salimian, S. Rastgar, *Mat. Sci. Eng. C-Mater.*, 34 (2014) 318.
17. A. Wong, M. Scontri, E.M. Materon, M.R.V. Lanza, M.D.P.T. Sotomayor, *J. Electroanal. Chem.*, 757 (2015) 250.
18. B. Liu, D. Tang, B. Zhang, X. Que, H. Yang, *Biosens. Bioelectron.*, 41 (2013) 551.
19. Y. Oztekin, Z. Yazicigil, A. Ramanaviciene, A. Ramanavicius, *Sensor. Actuat. B-Chem.*, 152 (2011) 37.
20. M. Chen, J. Xu, S. Ding, *Sensor. Actuat. B-Chem.* 152 (2011) 14.
21. X. Tan, Q. Hu, J. Wu, X. Li, P. Li, H. Yu, X. Li and F. Lei, *Sensor. Actuat. B-Chem.*, 220 (2015) 216.

22. D. Rao, Q. Sheng, J. Zheng, *Sensor. Actuat. B-Chem.*, 236 (2016) 192.
23. K.M. El-Khatib, R.M. A. Hameed, R.S. Amin and A.E. Fetohi, *Int. J. Hydrogen Energ.*, 42 (2017) 14680.
24. R.T. Kushikawa, M.R. Silva, A.C.D. Angelo, M.F.S. Teixeira, *Sensor. Actuat. B-Chem.*, 228 (2016) 207.
25. S. Shahrokhian, R. Salimiana, S. Rastgar, *Materials Science and Engineering C*, 34 (2014) 318.
26. F.L. Guzmán-Duque, R.E. Palma-Goyes, I. González, G. Peñuela, R.A. Torres- Palma, *J. Hazard. Mater.*, 278 (2014) 221.
27. E. Laviron, *J. Electroanal. Chem.*, 101 (1979) 19.
28. J. Guillon, J. Guillon, A. Laffont, J. Bruzeau, L. Rochet-Mingret, M. Bonnefoy, J. Bureau, *J. Chromatogr. B*, 719 (1998) 151.

© 2018 The Authors. Published by ESG (www.electrochemsci.org). This article is an open access article distributed under the terms and conditions of the Creative Commons Attribution license (<http://creativecommons.org/licenses/by/4.0/>).